Pergamon

PII:S0899-5362(99)00108-6

Journal of African Earth Sciences, Vol. 29, No. 3, pp. 429–447, 1999

0899-5362/99 $- see front matter

Depositional facies of the Cambrian Araba Formation in the Taba region, east Sinai, Egypt

A. EL-ARABY* and A. ABDEL-MOTELIB
Geology Department, Faculty of Science, Cairo University, Cairo, Egypt

ABSTRACT—A thick succession of Cambrian sediments is exposed in the Taba region, east Sinai, and subdivided into the Araba Formation and the overlying Naqus Formation. The vertical and lateral distribution of the Araba Formation in the Taba region provides an outstanding example of an overall retrograding sequence. Three distinctive units (I, II and III) are distinguished within this succession on the basis of depositional geometries, stratified patterns, sedimentary features and petrographic examinations. They record different depositional environments and each unit is distinguished by a particular facies association, which records processes characteristic of these environments. The lower unit (I) is dominated by five depositional facies (Ia-Ie) which belong to low sinuosity braided channels associated with floodplain fines and alluvial fans. Channel deposits are represented by tabular cross-bedded and horizontally stratified pebbly coarse-grained sandstones. The middle unit (II) reveals a relative sea level rise and is composed of fine- to coarse-grained sandstone, shale and mudstone with carbonate intercalations. From four depositional facies (IIa-IId), recognised facies (IIa, IIc and IId) are comparable to upper-lower shoreface and tidal channel environments. The fourth facies (IIb) is carbonate-dominated with trilobite tracks, and reflects deposition in the upper-middle intertidal flat. The latter facies (IIb) is subjected to intra-Cambrian karstification, which is deduced from the presence of macro- and microscopic fresh water calcite fillings, botryoidal Fe and Mn oxides and terra rossa. The uppermost unit (III) is shale-dominated from the inner shelf and is represented by two facies (IIIa and IIIb). Despite the general rise in sea-level in the Araba Formation, the uppermost facies (IIIb) points to a progradational-upward tendency in unit (III), and this is coeval with an increase in the percentage of interbedded fine-grained sandstones.

RÉSUMÉ—Les sédiments cambriens forment dans la région de Taba, Sinaï oriental, une épaisse séquence subdivisée en formation Araba et formation de Naqus, au-dessus. La répartition verticale et latérale de la formation Araba de la région de Taba donne un excellent exemple de séquence rétrograde d'ensemble. Trois unités (I, II et III) se distinguent dans la formation d'après la géométrie des dépôts, l'allure des strates, les caractères sédimentaires et les examens pétrographiques. Elles enregistrent des contextes de dépôt différents et chaque unité se distingue par une association particulière de faciès enregistrant les processus caractéristiques des environnements. L'unité inférieure (I) comprend cinq faciès (Ia-Ie) de dépôts de chenaux anastomosés peu sinueux avec des sédiments fins de plaine inondable et des cônes alluviaux. Les dépôts de chenaux sont représentés par des grès grossiers graveleux tabulaires à stratification oblique et horizontale. L'unité moyenne (II) montre une augmentation relative du niveau de la mer et se compose de grès fins à grossiers, de shales, de boues avec des intercalations carbonatées. Sur les quatre faciès de dépôt (IIa-IId) reconnus, trois (IIa, IIc et IId) sont comparables aux environnements côtiers (inférieur-supérieur) et aux chenaux de marées. Le quatrième faciès (IIb) est carbonaté, avec des traces de Trilobites, et reflète un dépôt en milieu plat intertidal supérieur-moyen. Il a été soumis à la karstification intra-cambrienne,

* Corresponding author
elaraby@main-scc.cairo.eun.eg (A. El-Araby)

déduite par la présence de remplissages de calcite macro- et microscopique à partir d'eau douce, d'oxydes de Fe et Mn botryoïdes et de terra rossa. L'unité supérieure (III), dominée par les shales de plateforme interne, est représentée par deux faciès (IIIa et IIIb). Malgré la montée générale de l'eau de mer dans la formation Araba, le faciès supérieur (IIIb) indique une tendance à la progradation vers le haut, en relation avec l'augmentation des grès fins interstratifiés.

(Received 26/5/98: revised version received 20/8/98: accepted 22/10/98)

INTRODUCTION

The present study is focused on the Early Cambrian Araba Formation at Wadi El-Mirakh, about 15 km to the west of the Taba-Nueiba road, and Wadi Tueiba, east Sinai (Fig. 1). The Cambrian strata are exposed at several localities in west central Sinai: the Um Bogma area, south Wadi Feiran and the Abu Durba area. At the eastern side of Sinai, the Cambrian sediments are recorded as faulted blocks along Taba-the Nueiba road (Abdel-Khalek *et al.*, 1992). A comprehensive documentation of the stratigraphy and sedimentology of the Cambrian rocks in Sinai have been discussed by Bauerman (1869), Barron (1907), Ball (1916), Kostandi (1959), Hassan (1967), Weissbrod (1969), Soliman and El-Fetouh (1969), Said (1971), Issawi and Jux (1982), Beleity *et al.* (1986), Bhattcharyya and Dunn (1986), Allam (1989), El-Sharkawi *et al.* (1990), Klitzsch (1990), Weissbrod and Perath (1990), El-Barkooky (1992, 1996), Abdallah (1992), Semtner and Klitzsch (1994), McBride *et al.* (1996), El-Kelani (1996), and others.

The name Araba Formation was given by Hassan (1967; in Said, 1971) to describe the Lower Palæozoic sediments in the Abu Durba area. It has been applied for regional use of the Cambrian strata in Sinai by Klitzsch (1990). In Sinai, the Araba Formation nonconformably overlies the Precambrian basement and conformably underlies the Naqus Formation. Weissbrod (1969) and Omara (1972) assigned an Early Cambrian age for the Araba Formation, while Issawi and Jux (1982) and Kora (1984) extend its age to cover the Cambro-Ordovician. Seilacher (1990) also gave an Early Cambrian age to the Araba Formation.

Along the study area, the surface exposures of the Lower Palæozoic sediments represented by the Araba and Naqus Formations are covered by a blanket of sedimentary strata, ranging in age from Early Cretaceous (Malha Formation) to Late Cretaceous (Galala, Wata and Sudr Formations). These sediments are followed by Palæocene (Esna Formation) and Eocene rocks (Thebes and Samalut Formations). They are locally overlain by Pliocene and Quaternary deposits (Abdel-Khalek *et al.*, 1992, 1993). At Wadi El-Mirakh, the Cenomanian Galala Formation forms the cap rock of the underlying Lower Palæozoic and Lower Cretaceous clastics (Fig. 1). The Araba Formation at the study area is distinguished by its red-brown-green colourations, low sand/shale ratio, carbonate interbeds and marine affinity, while the overlying Naqus Formation is characterised by its bright colourations, massive appearance, high sand/shale ratio, an increase in pebble content and dominantly continental depositional environments.

The objectives of this paper are to elucidate lithofacies, petrographic characteristics and sedimentological processes, as well as to interpret the depositional environments of the Araba Formation in the study area. Emphasis is placed on minor breaks and hiatuses in this succession.

DESCRIPTION AND INTERPRETATION OF LITHOFACIES

The Early Cambrian Araba Formation in the study area is dominated by siliciclastics: conglomerates, sandstones, mudstones and shales. Carbonate interbeds represent about 7% of the studied succession and they are discussed for the first time in the present study. The sampled section (70 m thick) at Wadi El-Mirakh can be subdivided into three units (Fig. 2), each represents a specific depositional system. The change in lithological parameters and sedimentary structures define the boundary between the units. These units reflect distinct changes in eustatic sea level, which excerises a major influence on sedimentation processes as well as on the amount and type of sediment influx. The different lithofacies have been petrographically examined to determine their characteristic terrigenous components, mineralogy, authigenic mineral phases and textural relationships. The sandstones are classified according to Pettijohn *et al.* (1973), based on their mineralogical composition. Thin sections containing carbonates were stained with Alizarin Red-S and K ferricyanide to aid in determining the Ca, Mg and/or Fe content of the carbonate minerals. In the following, the three studied units of the sampled section of the Araba Formation will be disccussed. Detailed descriptions and interpretation of the different lithofacies are given.

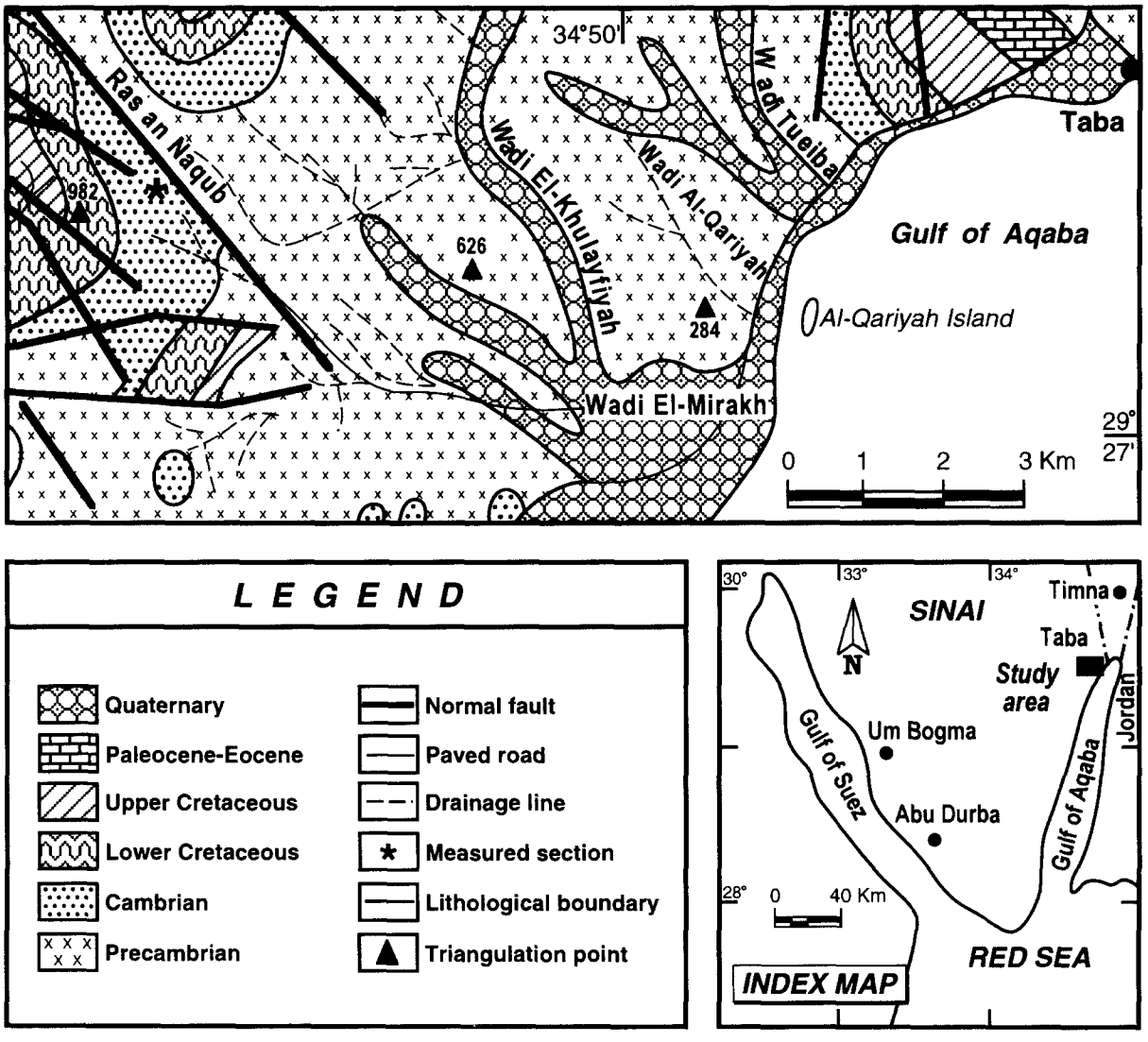

Figure 1. *Simplified geological map of the Taba region, Sinai, Egypt (based on Topographic map of Sinai, 1952; Abdel-Khalek* et al., *1992, 1993; Geological map of Sinai, 1994).*

Unit I

This unit constitutes the basal part of the examined section and is 27 m thick (Fig. 2). It has an unconformable irregular contact at the base which separates the Lower Palæozoic strata from the underlying Precambrian igneous and metamorphic rocks (Fig. 3A). The following lithofacies have been distinguished in unit I (i.e. bed Nos A1-A14, Fig. 2).

Facies Ia: disorganised matrix-supported conglomerates

Description. This facies occurs in the middle part of unit I (A5, Fig. 2). It consists of polymictic, matrix-supported, poorly sorted conglomerates (Fig. 3B). The lithoclasts range in size between 1 and 15 cm. They are mainly composed of subangular to rounded pebbles of quartz, rhyolite, granite, chert and laminated mudstone. The quartz pebbles exhibit pink, milky-white or amber-like colour. The clast shape is bladed to oblate. The basal part of this facies is ferruginous, while the upper one is siliceous. Most of the matrix consists of white siliceous sand with a subordinate clay content. Facies Ia lacks internal stratification, a graded/organised fabric and has a lower irregular boundary.

Interpretation. Facies Ia reflects deposition from cohesive debris flows where they move as dense viscous masses and the matrix strength is large enough to transport the lithoclasts (Miall, 1977; Chun and Chough, 1995; Collinson, 1996). As the flow decelerates, poorly sorted deposits floating in a matrix are formed. The lack of basal scour or clast imbrication may indicate laminar (non-turbulent) flow during sediment transport (Horton and Schmitt, 1996). These facies characteristics indicate that facies Ia represents alluvial fan deposits near the fan apex.

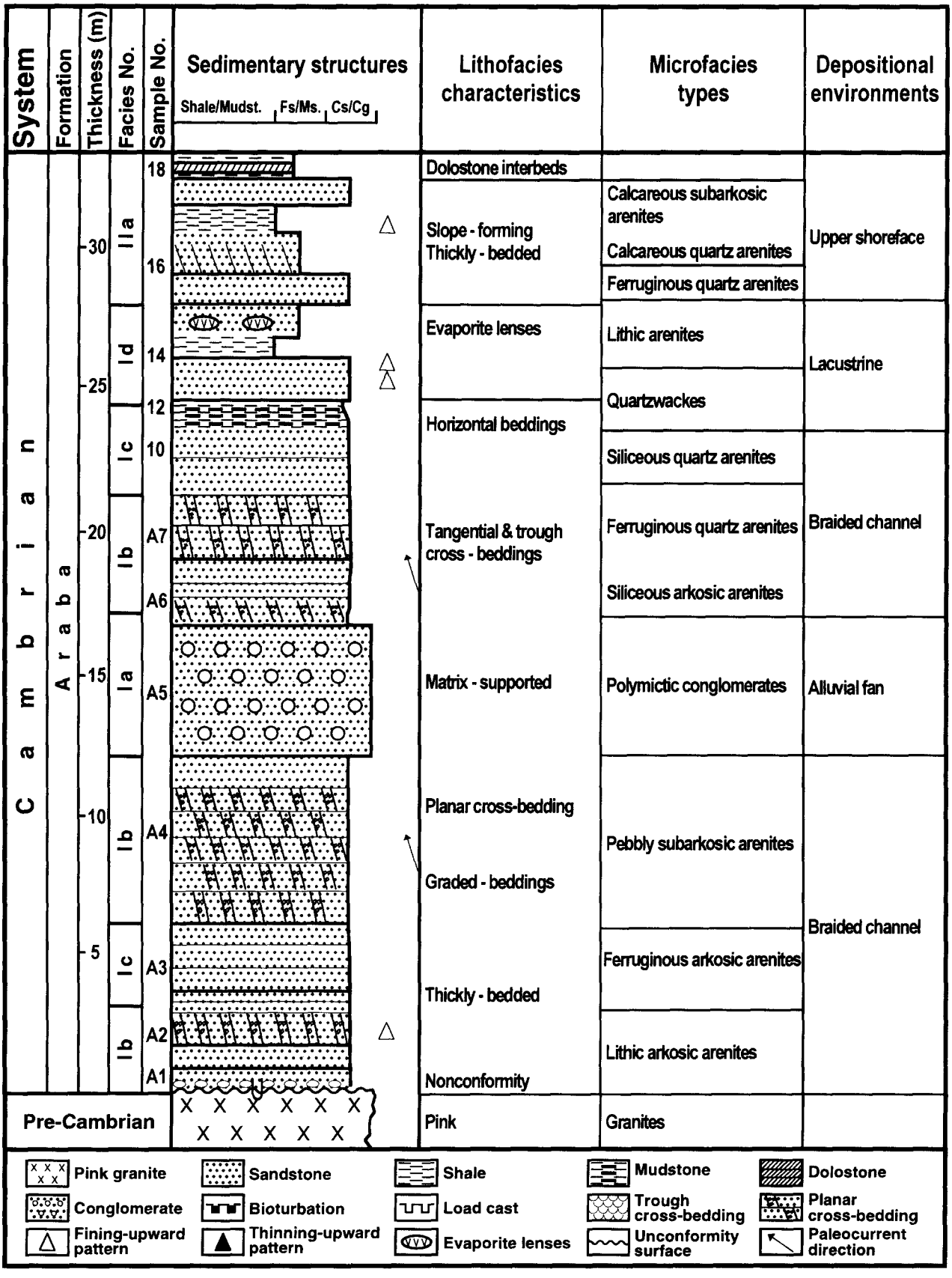

Figure 2. *Stratigraphical section exhibiting sedimentological characterisitics and environmental interpretation of the Araba Formation at Wadi El-Mirakh, Taba region, Sinai, Egypt (see Fig. 1 for loaction).*

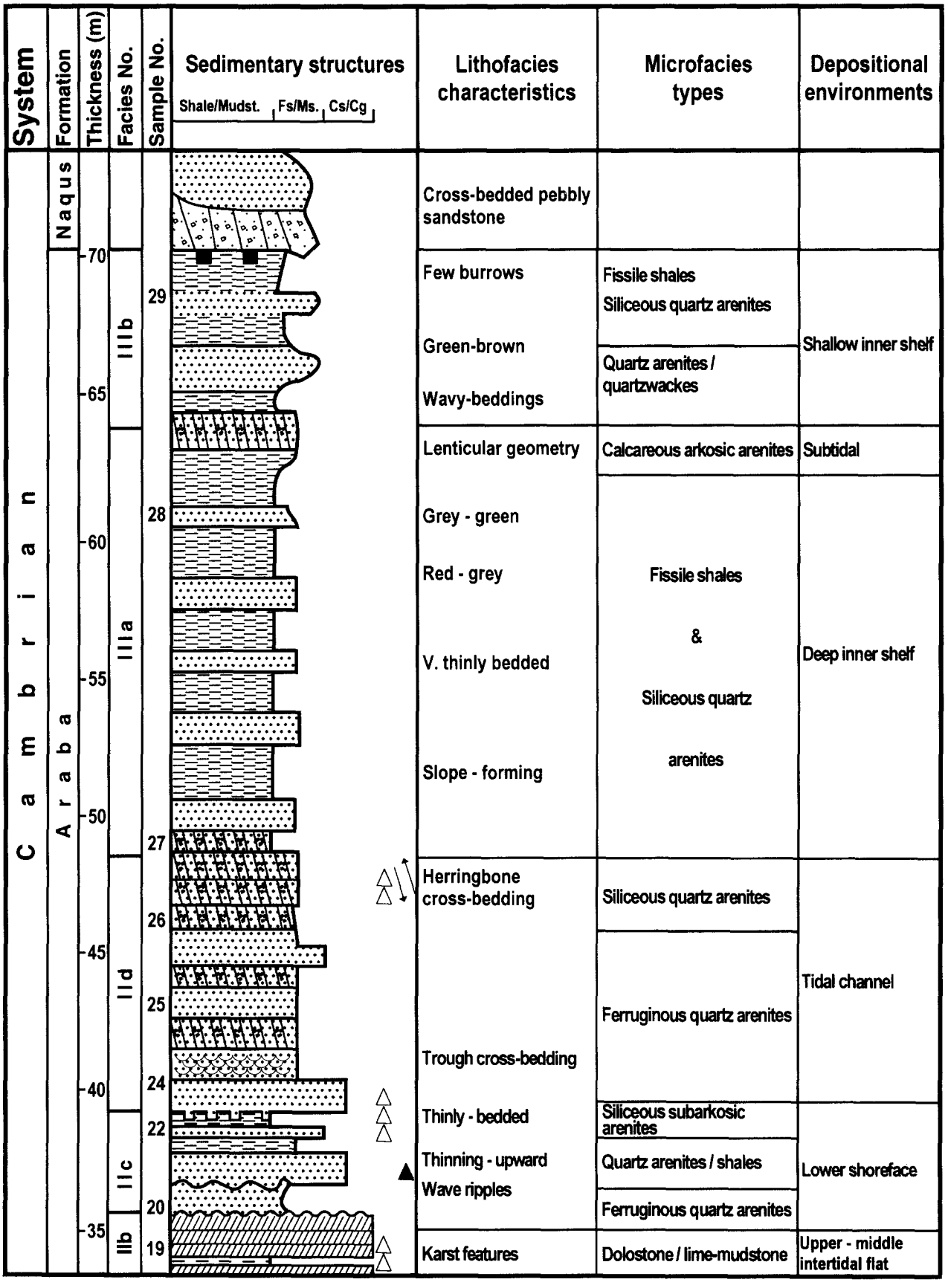

Figure 2. *continued.*

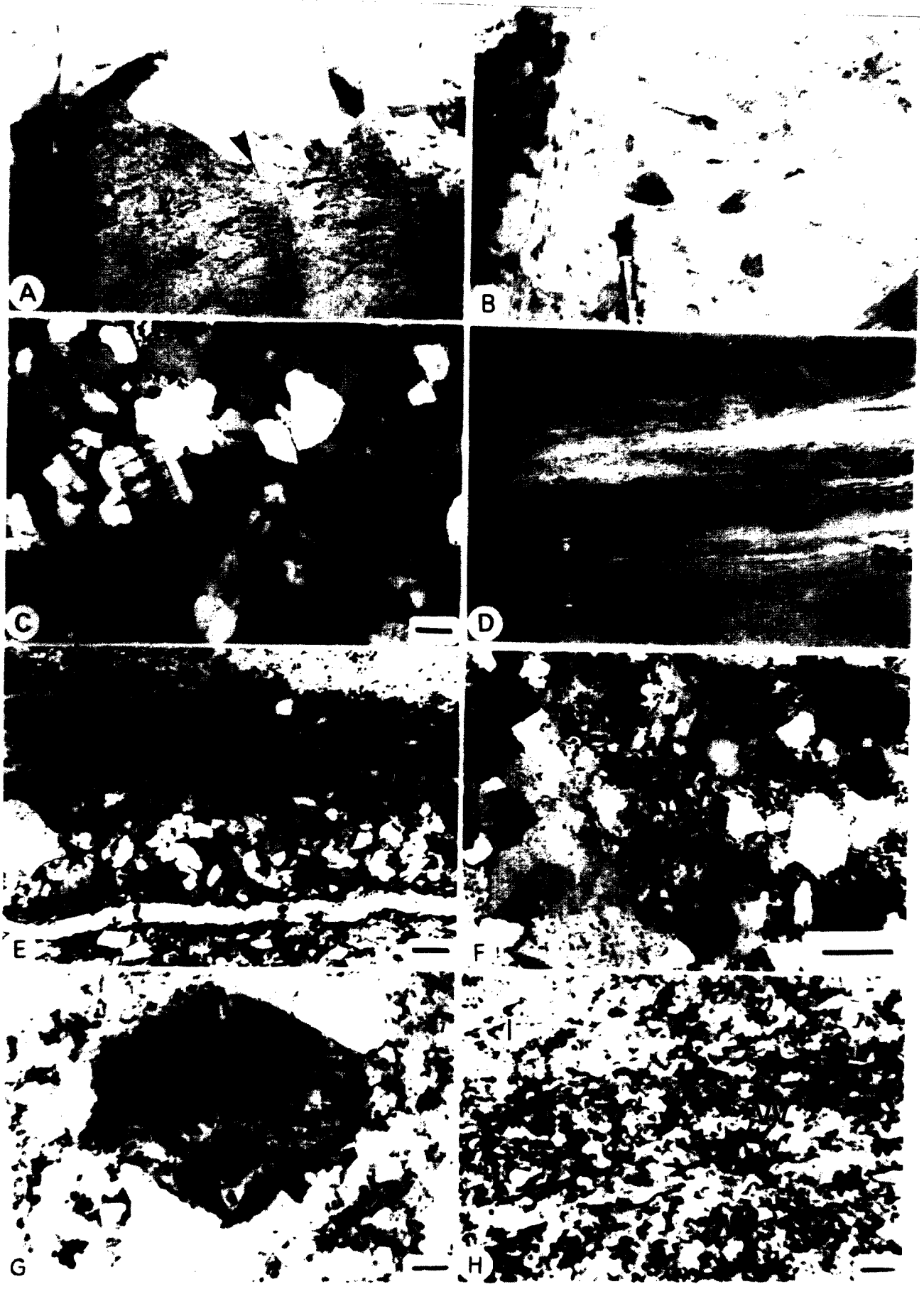
A
B
C
D
E
F
G
H
I

Facies Ib: cross-bedded pebbly sandstones

Description. This facies is widely distributed throughout unit I (A1, A3, A4, A6, A7, Fig. 2). It is composed of fine to coarse sand-sized quartz grains with a few scattered pebbles. Orthoclase grains are sparsely distributed in the sandstones. The facies colour varies between greyish-green, reddish-brown, pink, violet and pinkish-grey. The sandstones are moderately hard, partly ferruginous and/or micaceous. They reveal tabular and tangential cross-bedding. The sets range in height between 0.1 and 1 m and laminae thickness varies between 0.5 and 1 cm thick. Trough cross-bedding is less common and exists at the upper part of unit I (A7, Fig. 2). The trough width is up to 30 cm and their height varies between 10 and 15 cm. The cross-bedding cosets vary between 1 and 6 m in thickness. They either exhibit a fining-upward pattern, or show uniform grain size distribution. Cobbles of granites, gneisses, mudstones and chert are occasionally associated with elongated sand bodies.

Petrographically, this facies is built up of subrounded, poorly sorted and monocrystalline quartz grains, partly altered feldspars (i.e. microcline) and mica flakes. Authigenic kaolinite plates are locally present in the intergranular pore spaces. All constituents are cemented with siliceous cement, despite the presence of iron oxides as patches and spots. Facies (I b) is mineralogically classified as lithic arkosic to subarkosic arenites (Fig. 3C).

Interpretation. The facies characteristics such as unimodal palæocurrents, elongate sand bodies, low proportion of mud content and absence of lateral accretion deposits, point to low sinuosity braided river deposits (Fig. 4). The planar and trough cross-beds are generally produced by migration of medium-scale bedforms such as sand waves and dunes, respectively (Miall, 1977, 1985). The dunes usually occupy the deeper portions of channels, while sand waves are common in the shallower parts of the channels.

Facies Ic: horizontally stratified pebbly sandstones

Description. Facies Ic is recorded at the lower and upper parts of unit I (A3, A8, A9, A10, Fig. 2). It comprises pebbly coarse-grained, horizontally stratified, thickly bedded (0.3-1 m thick) sandstones of green, pinkish-grey, chocolate brown to violet colours. This facies displays cycles of medium- to coarse-grained, ferruginous/siliceous sandstones (30 cm thick) alternating with fine-grained sandstones (15 cm thick). The contact between them is sharp and wavy-rippled. The fine-grained sandstones have lenticular geometry and are repeated as lenses in horizontal and vertical directions. The sandstones are thinning-upward.

Petrographic examination of the fine-grained sandstones reveals their basic composition of poorly sorted, subangular-subrounded, monocrystalline, medium silt- to fine sand-sized quartz grains. Fine sand-sized plagioclase and mica flakes are present. All components are chiefly agglutinated with siliceous cement and locally with calcite cement, which partly replaces the quartz grains. Such mineralogical composition represents siliceous quartz arenites.

Interpretation. Parallel stratification in the sandstones is commonly related to deposition from an upper flow regime, and plane beds during the flood stage, which develops beneath flow of high velocity, or low depth (Miall, 1977). The horizontal stratifications are interpreted as deposits of subærial sheet floods (Horton and Schmitt, 1996), where they are interbedded with deposits of fine-grained sandstones.

Facies Id: homogenised mudstones

Description. It occurs in the lower part of unit I (A2, Fig. 2) and is built up of sheet-like, hard, ferruginous feldspathic, micaceous, grey mudstones/siltstones. The mudstones are about 15 cm thick.

Interpretation. Such deposits represent overbank deposits where they resulted from sheet flow of sediments over the channel banks during the flood stage. They are usually formed by suspension settling of organic-rich particles.

Facies Ie: heterolithic sandstones and mudstones

Description. This facies is 3.7 m thick and varies from sandstone- to mudstone-dominated beds at the top of unit I (A11-A14, Fig. 2). The mudstones are generally red and intercalated with white, grey,

Figure 3. *(A) Non-conformable basal contact between sandstones of the Araba Formation and the underlying Precambrian basement. Matrix-supported conglomerates of chert and quartz pebbles (arrow) demarcate this contact. (B) Matrix-supported, poorly sorted, polymictic, disorganised conglomerates; bed No. A5. (C) Subarkosic arenites reveal the presence of partly altered microcline grains characterised by cross-hatched twinning; bed No. A1, crossed polars. (D) Laminated white-grey sandstones, red siltstones and dark grey shales. Note the evaporite lenses and veinlets (arrows) are distributed at the same level at the top of the shales; bed No. A11. (E) Alternating laminae of quartz wackes and siltstones; bed No. A11, crossed polars. (F) Aggregates of secondary gypsum and anhydrite laths are locally present in the framework; bed No. A11, crossed polars. (G) Small-scale cavities outlined by algae and partly filled with micro-quartz crystals; bed No. A11, plane polarised light. (H) Alternated laminae of lithic arenites (l) and quartz wackes (w). Note the preferred orientation of the mica flakes; bed No. 14, plane polarised light. Scale bar = 400 μm.*

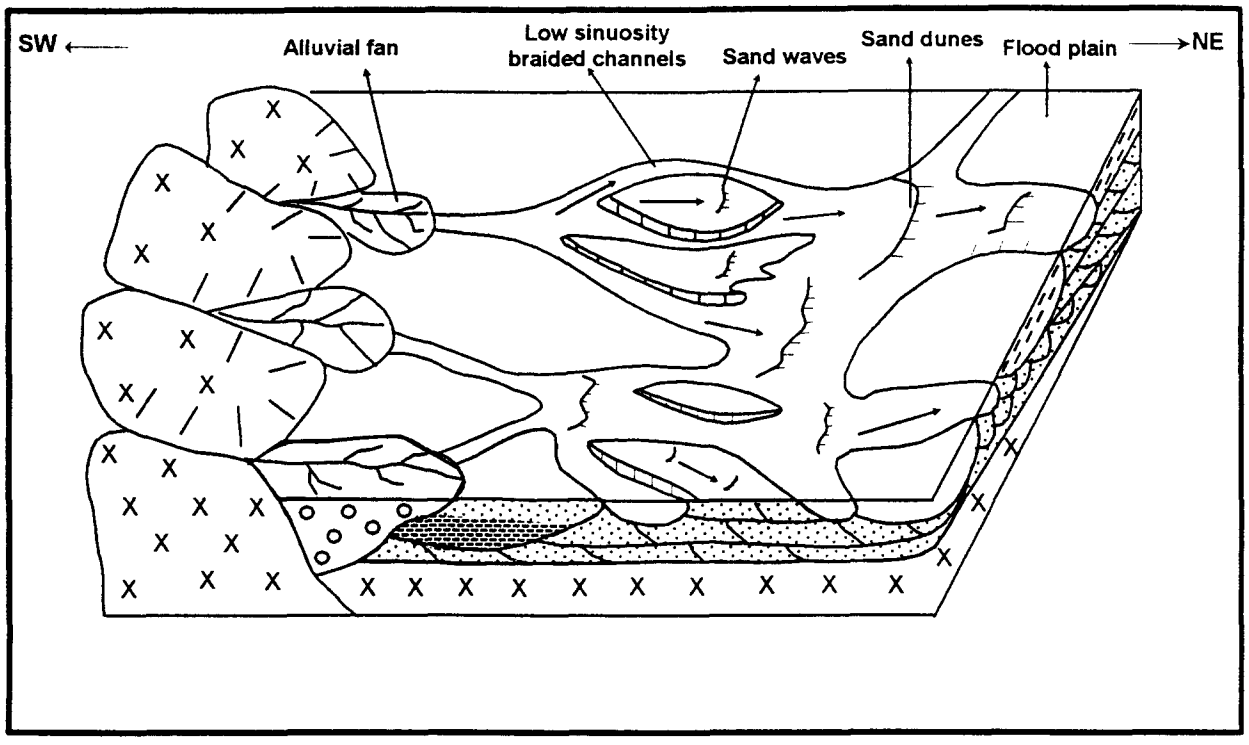

Figure 4. *Schematic block diagram of the alluvial subenvironments showing the distribution of different facies in unit I of the Araba Formation in the Taba region.*

green to red, very fine-grained sandstones (up to 2 cm thick). These sandstones are either found in the form of thin continuous beds, or display lenticular geometry in the mudstones. Small lenses of coarse-grained sandstones (2-20 cm in width) are recorded within the mudstones. At the lower part of this facies (A11, Fig. 2), dark grey mudstones associated with evaporite lenses are recognised. These lenses are scattered at the same level and their height and width reach up to 10 cm and 40 cm, respectively (Fig. 3D). At the upper part of facies Ie, red-coloured sandstones dominate where they exhibit horizontal and cross-laminations (A14, Fig. 2). These laminations are concomitant with the presence of strata-bound evaporite veinlets. Stationary toll marks are occasionally preserved on the bedding planes of sandstone beds. Very thin laminae, up to 3 cm thick, of pebbly coarse-grained sandstones with red argillaceous matrix are intercalated with fine-grained sediments. These laminae display scour-and-fill structures in the underlying sediments. The topmost part of this facies is intensively bioturbated and burrowed. The burrows are 20 cm long and 5 cm wide. Groove marks, 1-2 cm in width, are recorded on the upper irregular contact of this facies.

Petrographic study of the lower part of facies Ie reveals alternating laminae, up to 0.8 mm thick, of two different types (A11, Fig. 2). The first one consists of quartz wacke made up of subrounded, very fine sand-sized, monocrystalline quartz grains (Fig. 3E) and partly altered K-feldspar grains. The second type is siltstone being composed mainly of coarse silt-sized quartz grains. A few mica flakes, kaolinite plates and black organic material are present in this framework. Laths of anhydrite crystals and microcrystalline aggregates of secondary gypsum (Fig. 3F) are recognised. Some cavities outlined by algae are refilled with microcrystalline quartz crystals (Fig. 3G). Petrographically, the topmost bed (A14, Fig. 2) also exhibits two types of laminae, up to 2.6 mm thick (Fig. 3H). The first one is quartz wacke composed of very fine sand-sized quartz grains and mica flakes, which exhibit preferred orientation. The second type of laminae reflects lithic arenites, which is made up of subangular-subrounded, fine sand-sized, monocrystalline quartz grains with secondary constituents of very fine sand-sized K-feldspar and plagioclase grains, mica flakes and an argillaceous matrix.

Interpretation. The laminated sandstones and mudstones record episodic sedimentation and reflect seasonal variation in clastic supply. These sediments were deposited from shallow flow in an upper flow regime at the floodplain. The presence of this facies points to low sedimentation rates due to high velocity floodplain currents and low concentrations of suspended sediments at the flood peak (Reading, 1981).

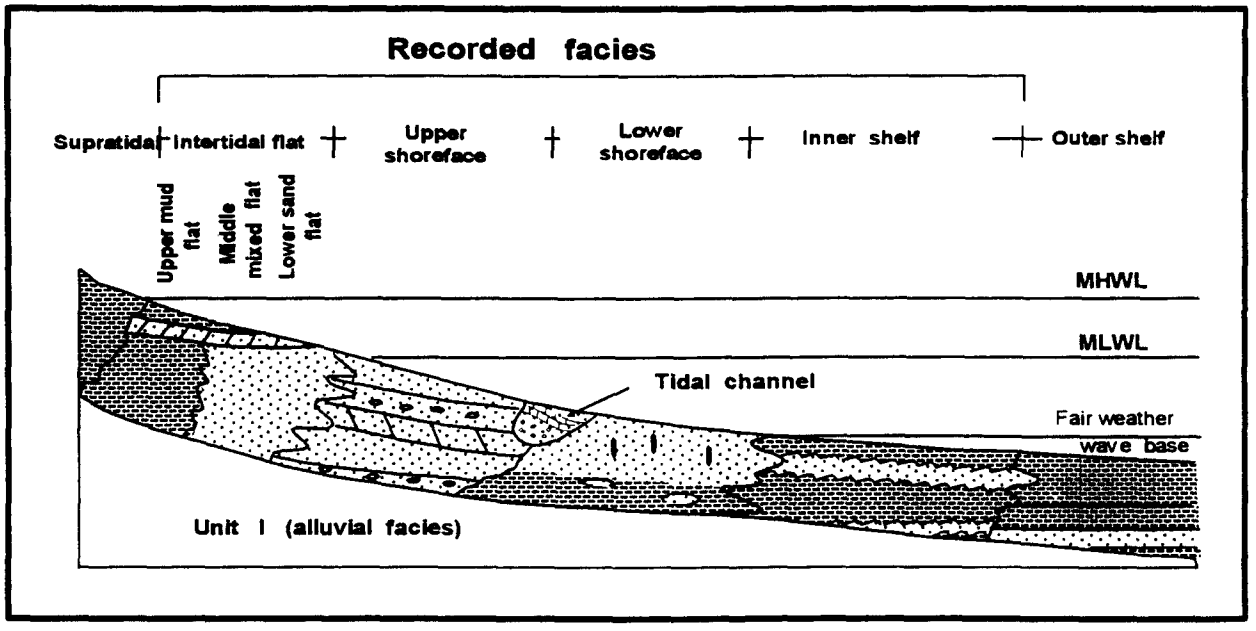

Figure 5. Schematic sketch summarising the subenvironment setting envisaged for the deposition of units II and III, Araba Formation, Taba region.

Silt and mud are deposited from suspension, while fine-grained sandstones are produced when peak flood currents are sufficiently strong to transport them. The occasional presence of internal fine laminations, small-scale cross-bedding and bioturbations are commonly recorded in this environment. Evidence of emergence are distinguished in the form of a reddening of these sediments, as well as secondary gypsum cement. The presence of stationary toll marks and erosional structures (i.e. groove marks) supports deposition at the floodplain, where they point to regions of intermittent subærial exposure and shallow water sedimentation affected by water level changes, respectively (Reineck and Singh, 1980).

Unit II

This unit conformably overlies unit I and is up to 25 m thick. It has horizontally stratified, pebbly, fine- to coarse-grained sandstones at the lower part, which are overlain by carbonate-dominated facies and thinly bedded sandstones, respectively. The cross-bedded sandstones constitute the uppermost part of unit II (i.e. bed Nos A15-A27, Figs 2 and 5).

Facies IIa: horizontally stratified sandstones

Description. It is basically composed of alternating ferruginous red and grey thinly to thickly bedded (2-30 cm thick), moderately hard, fine- to coarse-grained sandstones (A15-A18, Fig. 2). They display a fining- and thinning-upward pattern. Pebbles are sparsely distributed in the sandstones. At the lower part of this facies, planar cross-bedding is observed, where the sets are 10 cm in height and laminae thickness is about 3 cm. Upwards, there are rhythmic alternations of red and white, very fine-grained sandstones with wave-rippled tops, and mudstones (A16, Fig. 2; Fig. 6A). The basal part of these sandstones is cross-laminated, each is 2-10 cm thick and separated from the upper one by red pebbly manganiferous sandstones, which show tangential cross-bedding.

The upper part of facies IIa consists of intercalations of red, fine-grained sandstones and red to grey mudstones (Fig. 6B). Thin, black ferruginous/manganiferous dolostone beds, 5 cm thick, with moulds of fossils are intercalated with mudstones. Thinly bedded black to red ferruginous, pebbly, coarse-grained sandstones, 2-5 cm thick, are distinguished as well (A17, Fig. 2), where they attain 0.5 m in thickness. The topmost part of facies IIa consists of red mudstones and shales intercalated with fine-grained sandstones.

Petrographically, the lower part of facies IIa (A16, Fig. 2) is composed of subrounded to subangular, coarse silt- to fine sand-sized, monocrystalline quartz grains (Fig. 6C). Mica flakes, plagioclase grains, Fe oxides and zircon grains are sparsely distributed. This framework is cemented with calcareous cement and is classified as calcareous quartz arenites. The major component of the topmost part of this facies (A18, Fig. 2) consists of rounded, fine- to coarse-grained sand-sized, monocrystalline quartz grains. Chert, coarse sand-sized plagioclase and K-feldspar grains are common. All components are agglutinated by calcareous cement and the sandstone is classified as calcareous subarkosic arenite.

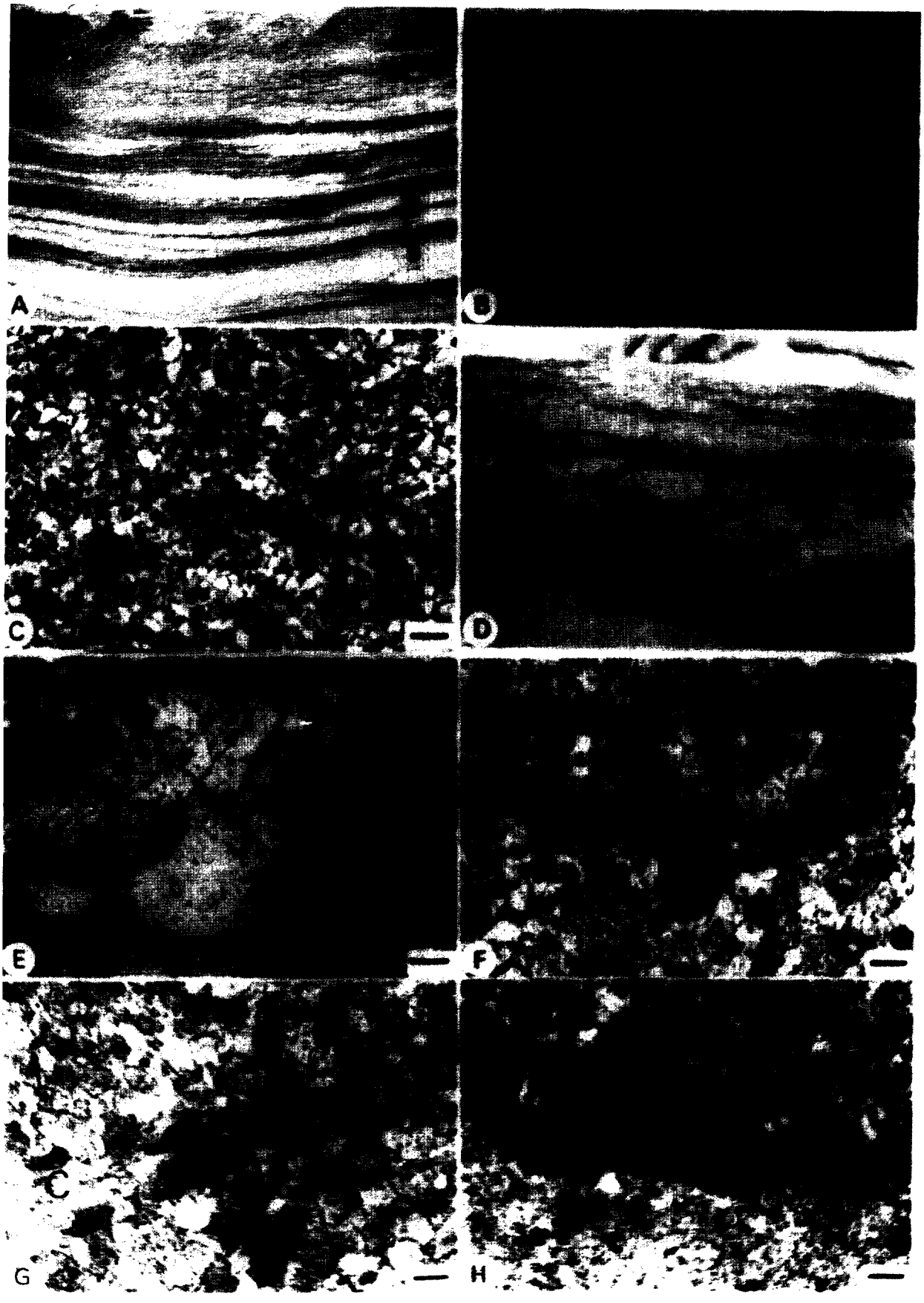
A
B
C
D
E
F
G
H

Interpretation. The fining-upward tendency, dominance of parallel laminations and fine-grained sandstones, weak bioturbations and presence of fossil moulds of facies IIa point to upper shoreface depositional environment (Johnson and Baldwin, 1996). The small-scale planar cross-bedding and reduced height and wavelength of the wave-rippled sandstones reflect a shallow water depth. These sedimentary structures record an interplay between wave and tidal processes which are characteristic of the upper part of the shoreface. The rhythmic pattern and the presence of intercalated carbonate beds in the middle part of this facies reflect alternate periods of carbonate and siliciclastic deposition, which supports an overall transgressive shoreline system. The graded interbedded, erosively-based, pebbly coarse-grained sandstones of this facies are deposited during storm periods and they are common in the upper shoreface facies (Einsele, 1992).

Facies IIb: carbonate-dominated

This facies varies in thickness between 2.5 and 4.5 m. It is composed of interlaminated calcareous sandstones/mudstones, dolostones and shales. The lower part of facies IIb is 1.5-2.5 m thick and composed of interbedded calcareous sandstones, grey-red, thinly laminated mudstones and dolostone interbeds, up to 2 cm thick. The mudstones are wave-rippled, with a wavelength of about 10 cm. The upper part of this facies, 1-2 m thick, is dominated by dolostones (A19, Figs 2 and 6D). They generally show a thickening-upward pattern and internal parallel stratification. Occasionally, these laminations have a stromatolitic appearance.

Dolostone beds are light grey and thickly-bedded, up to 15 cm in thickness. Manganese dendrites and cavities, 2 cm in diameter, filled with sparry calcite cement, occur. Upwards, red dolostone beds are interbedded with powdered terra rossa of red mudstones. Examination of polished surfaces of carbonate beds indicates that these rocks are dark grey, very thinly-laminated and karstified at the base, followed by thin red dolostones beds, up to 1 cm thick. Trilobite tracks are observed in some dolostone beds. These beds have a crinkled appearance and are interlaminated with red and grey mudstones, up to 0.5 cm thick. The recorded laminated terra rossa is composed of dark brown-red powdered calcareous mudstones and Fe/Mn oxyhydroxides. Clay cutans, cracking and caliche-like encrustations of calcite and Fe sesquioxides on muddy fragments and dolobreccia are recognised in these laminae. Microcracks extend from the terra rossa into the underlying carbonate interbeds. Bioturbations and mud cracks occur near the top of this facies, and they are concomitant with an increase in clastic/carbonate ratio, where red sandy dolostones and calcareous sandstones dominate. Quartz pebbles are dispersed in the topmost dolostone beds. Petrographic characteristics of the dolostone and sandstone beds allow the separation of two microfacies.

Calcitic dolostone

It forms a mosaic of tightly interlocking, coarse crystalline ferroan dolomite rhombs with equigranular texture. However, two types of dolomite rhombs are distinguished. The first one is made up of xenotopic, cloudy dolomite rhombs ranging between 40 and 70 μm in diameter. The second type is more pervasive and consists of hypidiotopic-idiotopic dolomite rhombs (0.2-0.6 mm in diameter). They display a cloudy appearance due to the presence of brown inclusions of Fe oxides, clays or organic matter and they lack zoning (Fig. 6E). Occasional zoning is observed where an outer rim of non-ferroan dolomite is developed. These rhombs have irregular or planar contacts. The coarse crystalline dolomite rhombs are selectively dedolomitised, where non-ferroan calcite crystals follow the zoning of the precursor rhombs. Non-selective dedolomitisation is also recorded where the entire rhombs are entirely calcitised. The framework is occasionally cross-cut by stylolite seams. They are filled with non-ferroan sparry calcite and Fe-rich clay residuum. In thin section, most of the replacive, coarse-grained, euhedral calcite crystals are not tightly linked with stylolite seams. Very fine sand-sized quartz grains are sparsely distributed in the framework and exhibit an upward increase towards the top. They occasionally constitute thin laminae parallel to bedding planes. Very

Figure 6. *(A) Rhythmic alternation of red and white very fine-grained sandstones and siltstones. Note the presence of tangential cross-beddings (arrow); bed No. A16. (B) Stratified sandstone and dolostone beds (ledge-forming) interlayered with red mudstone. Note the existence of black manganiferous laminae near the top; bed No. A18. (C) Calcareous quartz arenites display partial replacement of quartz grains by calcite cement. Iron oxides are sparsely distributed in the framework; bed No. A16, plane polarised light. (D) Dark grey and red massive dolostones at the base, followed by wave-rippled, karstified algal dolostones at the topmost part of facies IIb; bed No. A19. (E) Mosaic of fine, xenotopic, cloudy dolomite rhombs (d1) and coarse, recrystallised, hypidiotopic rhombs (d2). Note the selective dedolomitisation in the form of non-ferroan calcite; bed No. A19, plane polarised light. (F, G) Brecciated dolostones along the bedding planes. The dolobreccia are encrusted by Fe and Mn sesquioxides and calcite cement (c); bed no. A19, plane polarised light. (H) Preservation of an algal (microbial) mat forming microscopic connected domal mounds. Note the presence of quartz grains and Fe oxides along their upper surface; bed No. A19, plane polarised light. Scale bar = 400 μm.*

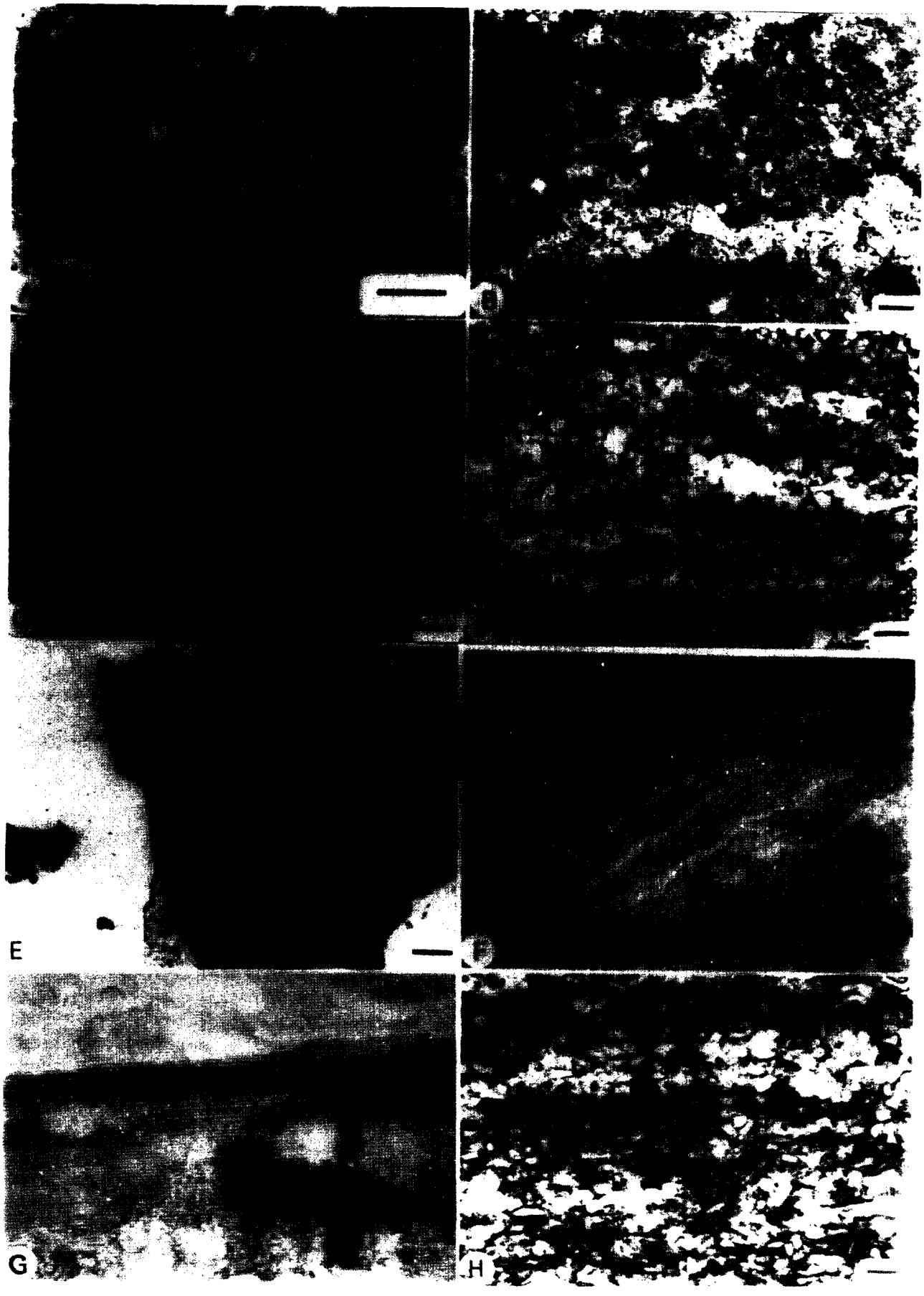
E
G
H

few anhydrite crystals are also scattered in the cementing material.

The profile of the upper part of facies IIb reveals diagnostic petrographic characteristics. Near its base, *in situ* brecciation is recorded by a widening of solution planes, such as shrinkage cracks and bedding planes (Fig. 6F). The resulting cracks are filled with dispersed idiotopic-hypidiotopic, cloudy dolomite rhombs, Fe and Mn sesquioxides and clayey earthy material, as well as non-ferroan sparry calcite cement (Fig. 6G). Above this occurs parallel algal (microbial) laminae, up to 0.5 mm thick (i.e. algal laminites) with a microscopic form of connected domal mounds (Fig. 6H). Very fine sand-sized quartz grains and Fe sesquioxides are dispersed within the troughs between these microscopic algal mounds. In the middle part of this profile, subrounded vugs and cavities, 1-1.5 cm in diameter, are locally rimmed by Fe oxides and filled with non-ferroan sparry calcite cement (Fig. 7A), Fe oxides and/or zoned coarse crystalline, partly calcitised, hypidiotopic-idiotopic dolomite rhombs. Besides this, elongated cavities are observed in the form of parallel laminae (i.e. laminoid fenestrae), up to 0.4 mm thick, undulating and locally vertical and branching (Fig. 7B). They are encrusted with Fe oxides, algal filaments and clayey material, and filled with sparry calcite cement, Mn and Fe glæbules and/or zoned dolomite rhombs. Near the top of the recorded profile, quartz grains become obviously pervasive.

Calcareous quartz arenites

This type occurs at the top of facies IIb. It is composed of very fine sand-sized, angular to subrounded quartz grains. They exhibit low sphericity and poor sorting, as well as tangential and concavo-convex contacts. The quartz grains are partly or completely coated by a thin brown rim of Fe oxides. Very fine spots of Fe oxides are also recorded filling the intergranular pore spaces. This framework comprises a closed packed fabric. These grains are chiefly cemented by non-ferroan calcite cement, which reveals partial replacement with these grains (Fig. 7C).

Interpretation. The presence of interlaminated dolostone, fine-grained siliciclastic beds, trilobite tracks, algal (microbial) mats, bioturbations, rootlets and laminoid fenestrae reflect deposition by weak currents and wave action and point to restricted platform and middle to upper intertidal flat depositional environments. Calcareous sands and muds of tidal sediments are cemented early and therefore have a particularly high preservation potential. The growth and preservation of algal (microbial) mats are favoured by hypersaline waters in intertidal and subtidal zones (Einsele, 1992). The associated voids (e.g. vugs and laminoid fenestrae) are generated by crinkling when the sediments are exposed to air, or by gases due to decomposing organic matter. Evidence of emergence and contact with meteoric water, such as mud cracks and karstification, are recorded near the top of the upper part of facies IIb. The preservation of fine-scale laminations suggests that these areas are frequently exposed and therefore unsuitable for marine burrows, which would destroy such laminations. Also, the presence of planar algal laminites indicates deposition on protected shorelines which have low relief (Tucker and Wright, 1990). The alternation between algal laminae and carbonates reflects fluctuating periods of wet and dry climates (Rupple and Cander, 1988). The coexistence of thin sandstone laminae is attributed to storm surges. Their presence at the top of the algal laminae resulted from clastic influx at the end of wet periods.

A meteoric-marine mixing zone model is interpreted for the present late diagenetic dolomite rhombs. This model is expected to develop during major regressive periods (Tucker and Wright, 1990), and reflects a period of karst development (Morrow, 1982). The Mg^{2+} source is chiefly attributed to seawater and the source of Fe^{2+} for the ferroan dolomite rhombs is related to shale diagenesis and/or enrichment of the original environment in Fe and organic clays. The dolomitisation process is expected to occur before burial because the dolostone beds are parallel to the bedding planes. The local presence of Fe glæbules is related to pedogenic oxidation during an early diagenetic stage. On the other hand, a dedolomitisation process is favoured by the influx of meteoric water during the regressive period and the development dissolution cavities (Theriault and Hutcheon, 1987). From the petrographic investigation, the dedolomitisation partly occurs along stylolites, which are commonly the result of burial

Figure 7. *(A) Subrounded cavities are locally rimmed by Fe oxides (arrows) and filled with selectively calcitised (c), coarse, hypidiotopic-idiotopic, zoned dolomite rhombs; bed No. A19, plane polarised light. (B) Elongated and undulating laminoid fenestrae parallel to the laminae planes, rimmed with Fe oxides and filled with sparite cement; bed No. A19, plane polarised light. (C) Calcareous quartz arenites; bed No. A19, plane polarised light. (D) Alternated laminae of siliceous quartz arenites and ferruginous siliceous siltstones; bed No. A26, plane polarised light. (E) Calcareous arkosic arenites. Note the presence of partly altered feldspar grains (k) surrounded by calcite cement (c); bed No. A29, crossed polars. (F) Green shales exhibit contorted laminations in the upper part of unit III of the Araba Formation; bed No. A29. (G) Sharp planar contact separates the upper green shales of the Araba Formation and the overlying sandstones of the Naqus Formation; top bed No. A29. (H) Siliceous quartz arenites display a parallel orientation of black mica flakes; bed No. A29, plane polarised light. Scale bar = 400 μm.*

diagenesis. Hence, the dedolomitisation process is partly related to meteoric water influx associated with over-burden pressures (Kenny, 1992). It is also observed that dedolomite rhombs are cross-cut by stylolites, which confirm that meteoric water entry during a subærial exposure event prior to overburden, is also responsible for dedolomitisation process. The above mentioned evidence of emergence through facies IIb point to the presence of diastems through the studied section.

Facies IIc: thinly to thickly bedded sandstones

Description. Facies IIc reaches up to 4.3 m thick (A20-A23, Fig. 2) and commences with thickly bedded, pebbly, white to greenish-yellow, partly glauconitic, medium-grained sandstones in intervals up to 1 m thick. They reveal a thinning-upward trend. Thin interbeds of red ferruginous mudstones are intercalated with the sandstones. The intervals of intercalation vary in thickness between 0.20 and 1 m. Stratabound Mn layers of pyrolusite composition are recorded as thin beds, 5 cm thick, or as lenses at the top of sandstones. The topmost part of these lower sandstones is bioturbated and has an upper wave-rippled contact. It is followed by a thin bed, 0.3 m thick, of red to black, pebbly, coarse-grained sandstones. Consequently, the middle part of facies IIc is represented by thinly bedded, 2-3 cm thick, red to yellow sandstones intercalated with thin laminae, 1 cm thick, of green fissile shales which exhibit a wave-rippled contact with the sandstones. Shales dominate in the upper half of this part. The uppermost part of facies IIc is built up of grey, friable, moderately hard, fine-grained sandstones. They display tangential cross-bedding, where the set height is 20 cm and the laminae thickness is up to 3 cm thick. Black heavy minerals concentrate along the cross-bedding planes. Upwards, there are red to grey, fissile shales which reveal convolute bedding and include boudins of white sandstone.

Petrographically, the upper part of facies IIc (i.e. A23, Fig. 2) is classified as siliceous subarkosic arenite. It is chiefly composed of subangular-subrounded, coarse silt- to fine sand-sized, monocrystalline quartz grains. Fine sand-sized plagioclase and microcline grains are common. Mica flakes, clay minerals and anhydrite laths are distinguished in the framework. All components are lumped with siliceous cement.

Interpretation. The vertical sequence context of facies IIc, together with the pervasive decrease in grain size, increase in bioturbations, dominant planar cross-laminations and small-scale tangential cross-bedding, argue for an origin in the lower shoreface suite (Einsele, 1992). The sedimentary structures reflect the influence of tidal currents and storm-induced coastal flow, which characterise this suite (Johnson and Baldwin, 1996). The evenly laminated sandstones are produced by heavy storms, which eroded sands from the upper part of the beach and transfered them into suspension in turbulent water where they are settled down in deeper parts (Reineck and Singh, 1980). The recorded convolute bedding in shales and fine-grained sandstones are common features on the steeper slopes of sand bars in a tidal environment. The presence of burrowing reflects fair-weather periods to allow faunal activity in this part. This is accompanied by small-scale cross-bedding and wave-rippled cross-laminations, which point to deposition at least above the storm wave base (Ainsworth and Crowley, 1994).

Facies IId: cross-bedded sandstones

Description. This facies is characterised by a prevalence of cross-bedded fine- to coarse-grained sandstones (A24-A27, Fig. 2) and attains a thickness of about 9.3 m. It starts with pebbly coarse-grained sandstones, up to 1 m thick. They reveal graded bedding and are thickly bedded, where the bed thickness is about 15 cm thick. They have load structures with the underlying shales. Upwards, trough cross-bedding becomes common where the width and height are up to 1 m and 0.3 m, respectively. They are followed by planar cross-bedding, which display set height and laminae thickness up to 15 cm and 2 cm, respectively. Graded bedding is recognised along these laminae, where pebbles are dispersed at their base and mudstones dominate upwards. These sandstones are overlain by thin intercalations of yellow, white and grey fine-grained sandstones and red mudstones in intervals up to 0.4 m thick. Horizontal and inclined micro-burrows are recorded in the grey sandstones, where they are filled with mudstones. Thin laminae of green fissile shales, 5 cm thick, coexist with these intercalations. At the topmost part, herringbone cross-bedded, fine- to medium-grained sandstones are distinguished, where the set height and laminae thickness reach up to 35 cm and 2 cm, respectively. Clay drapes and Mn nodules are concentrated along these laminae planes.

Petrographically, the framework of the upper part of facies IId is built up of alternated laminae, 0.45 mm thick (A26, Fig. 2). The first laminae type represents the siliceous quartz arenite class, which is basically built up of monocrystalline, fine sand-sized quartz grains and reveals a closed packed fabric (Fig. 7D). They are cemented with siliceous cement and include unidentified clay minerals in the

intergranular pore spaces. The second type of laminae is made up of siliceous siltstones and consists of coarse silt to very fine sand-sized quartz grains, which display an open fabric cemented by siliceous material. Mica flakes, feldspar grains and argillaceous matrix are recorded as well in the framework.

Interpretation. The characteristics of the fining-upward succession of facies IId suggest tidal channel deposits which begin with an erosional base with relatively coarse lag deposits (A24, Fig. 2). They are overlain by medium-scale unidirectional trough and planar cross-bedding. At the top, bidirectional planar (herringbone) cross-bedding becomes dominant (A27, Fig. 2). Trough and planar cross-bedding resulted from the migration of dunes and sand waves, respectively, which usually cover the subtidal part of the depositional bank (Johnson and Baldwin, 1996). The association of clay drapes on the herringbone cross-bedded sand laminae point to lateral migration of the tidal channels. The fall-out from these fine-grained suspended sediments is introduced during the slack water period of the tidal cycle.

Unit III

This unit constitutes the upper part of the Araba Formation in the Taba region and attains a thickness of 21 m. The following two lithofacies are differentiated in unit III: the lower one is built up of shales and fine-grained sandstones; and the upper lithofacies is shale-dominated (i.e. bed Nos A28-A29, Figs 2 and 5).

Facies IIIa: grey-brown shales to fine-grained sandstones

Description. It reaches up to 15 m in thickness and is characterised by a predominance of slope-forming, reddish-brown to grey shales ranging in thickness between 0.3 and 0.8 m. Green patches coexist with brown shales. They are interlaminated with grey to green, siliceous, fine-grained, sharp-based sandstones, up to 3 cm thick. Green nodules of clay minerals, 2 cm in diameter, are recorded in the sandstones (A28, Fig. 2). The uppermost bed of this facies consists of burrowed red sandstones with dispersed yellow colourations, 0.5-1 m thick. They are overlain by fine- to medium-grained sandstones. They are thinly laminated, 5 cm thick, and include intervals of planar cross-bedded sandstones, up to 15 cm thick. A few burrows are locally recognised along the upper contact of this facies. Occasionally, facies IIIa is separated from the overlying facies by green shales interlaminated with grey-white, fine-grained sandstones in intervals up to 1 m thick. They display flaser bedding at the lower part and are followed by pebbly, arkosic, planar cross-bedded sandstones, which show lenticular geometry. The set thickness is up to 20 cm thick and it exhibits graded bedding. Petrographically, the sandstone framework is basically composed of medium sand- to pebble-sized, monocrystalline quartz grains. Chert, partly altered plagioclase and K-feldspar grains are distinguished. Zircon grains are common and all components are agglutinated with siliceous and calcareous cement. They are classified as pebbly calcareous arkosic arenites (Fig. 7E).

Facies IIIb: green-dark grey shales-dominated

Description. This facies, 6 m thick, comprises green to dark grey, partly reddish-brown-violet, fissile shales, 0.3-2 m thick. Locally, their upper part displays small-scale contorted laminations and slumps (Fig. 7F). The shales are interbedded with thin beds, 3-20 cm thick, of grey-white, fine- to medium-grained sandstones. Wave-rippled sandstones are recognised over short intervals in the middle part of this facies, and thin discontinuous flaser bedding of green shales coexist with sandstones. Small cross-laminations are developed at the uppermost sandstones, where the set thickness is 3 cm. The upper contact of facies IIIb with the overlying Naqus Formation is sharp, despite a local few burrows that are distinguished along this surface (Fig. 7G). Petrographic examination of the sandstones shows that their framework is chiefly built up of subangular-subrounded, monocrystalline quartz grains. A few chert and fine sand-sized feldspar grains are present. They reveal a closed packed fabric and are classified as siliceous quartz arenites (Fig. 7H). The framework of some examined beds exhibits alternated laminae, 150 μm thick, of siliceous quartz arenites interlaminated with quartz wackes.

Interpretation of unit III. The preponderance and continued preservation of clay-grade sediments of unit III are consistent with deposition at a slow rate and below the fair-weather wave base (Ainsworth and Crowley, 1994; Prave *et al.*, 1996). The association of these sediments with the high energy event beds of facies IIIa tends to suggest that they were affected by storm-generated currents. The interlaminated, thin, sharp-based, centimetre-thick sandstones reflect episodic storm deposits. The lack of graded bedding in these laminated sandstones suggests deposition by turbulent waters in a deeper environment. The increase in thickness of coarse-grained sediments and the concomitant association of wave-rippled structures in facies IIIb suggest deposition above the effective storm wave base in an offshore marine setting, under increasingly higher

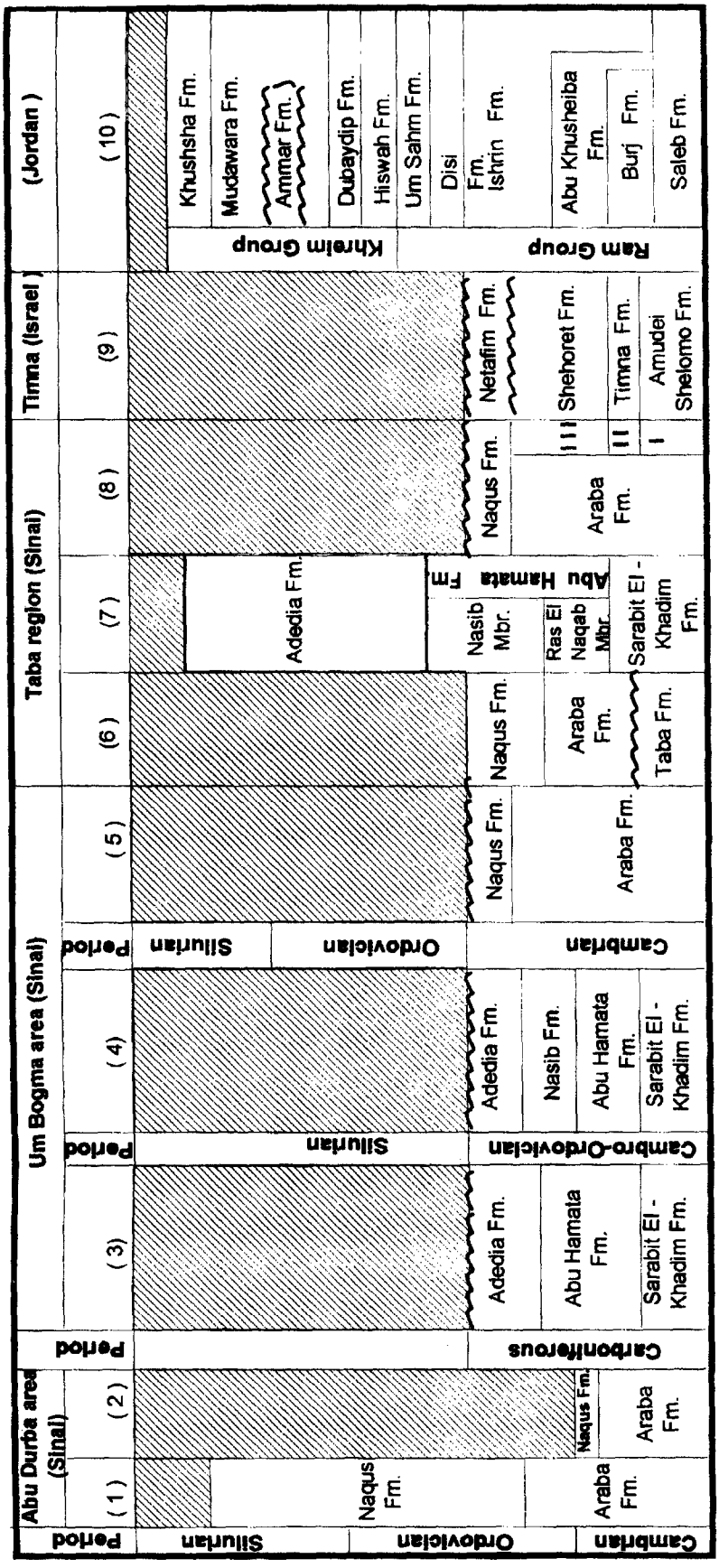

Figure 8. Correlation chart of the Lower Palæozoic lithostratigraphical units in Sinai and adjacent countries. 1: Issawi and Jux (1982); 2: Klitsch (1990); 3: Soliman and El-Fetouh (1969); 4: Kora (1984), El-Shahat and Kora (1986); 5: Abdel-Motelib (1996); 6: Said and El-Kelani (1988); 7: Kora (1991); 8: present study; 9: Weissbrod and Perath (1990); 10: Abed et al. *(1993).*

energy conditions. They reflect deposition in areas relatively near to the coast (Reineck and Singh, 1972). In contrast, the dominance of mudstones and the thinning of sandstones in facies IIIa implies deposition in a setting experiencing far fewer high energy events (Prave *et al.*, 1996). Facies IIIb displays a coarsening-upward trend relative to facies IIIa and points to progradation of proximal offshore marine deposits (facies IIIb) over distal deeper marine deposits (facies IIIa). The storm-deposited sandstones of the lower facies are usually followed by a long period of quiescence, which allows a thick succession of mud to be deposited, reflecting the greater water depths of the deep inner shelf environment. Facies IIIb reflects that wave-driven reworking forms oscillation ripples on the top of graded sandstone beds as soon as the storm currents subside (Einsele, 1992), and these features indicate a shallow inner shelf suite. The occasionally recorded flaser and lenticular bedding of the cross-bedded sandstones between the two facies of unit III reflects alternating conditions of sand deposition with others of slack water to allow fine-grained deposition. Such conditions point to formation in subtidal zones (Reineck and Singh, 1980). The recorded deformational features, such as slumps and contortions in facies IIIb, are contemporaneous with occasional rapid deposition in this domain. The presence of burrows at the top of unit III suggests fair-weather conditions to allow faunal activity. This unit is followed by a diagnostic eustatic sea level fall, which is accompanied by the deposition of the siliciclastic-dominated Naqus Formation under a fluvial regime.

REGIONAL CORRELATION

Northeast Africa formed a stable subsiding shelf at the northern margin of the Nubian Shield through most of the Early Palæozoic. The sedimentation processes were controlled during Cambro-Ordovician times by tectonic movements, whereas eustatic control predominated during the Silurian (Semtner and Klitzsch, 1994). The Precambrian crystalline basement of Sinai and the Eastern Desert of Egypt belong to the East Sahara Craton and the Arabo-Nubian Shield. They have undergone various intensive crustal deformations during the Pan-African orogenic event (*ca* 700 Ma; Stern and Kroner, 1993). The rapid growth of the north African Plate and Sinai had started by the end of the Pan-African, where Sinai, and the Eastern and Western Deserts were parts of Gondwana at that time (Morgan, 1990).

The Lower Palæozoic sediments of the Taba region, as well as of the adjacent territories of Israel, Saudi Arabia, Jordan and Egypt, are known as lower part of the Nubian Sandstone, which is of Cambrian-Cretaceous age. This term has become obsolete and has been replaced by many formal subdivisions of more well-defined ages. The continuity of lithological units from northern Africa to the Middle East attests to their common tectonic and depositional ancestry (Husseini, 1991). During the Cambrian, the sea transgression covered Jordan, southern Israel and Sinai. The Taba region represents the transitional zone between the open marine facies of southern Israel and Jordan in the northwest, and the more continental facies with less marine invasions towards the southwest (Um Bogma and Abu Durba areas). The Lower Palæozoic strata in Sinai are subdivided into the Araba Formation, of Early Cambrian age, and Naqus Formation, of probably Late Cambrian age (Klitzsch, 1990). The present authors have preferentially used the name Araba Formation to describe the Lower Cambrian rocks in the study area because it is suitable for regional correlation in Sinai and the Eastern Desert. The investigated Araba Formation in the Taba region was deposited under fluvial to near shore and inner shelf marine environments. The authors subdivided the formation into three main units. The lower one deposited in a fluvial regime is equivalent to the Sarabit El-Khadim Formation of Soliman and El-Fetouh (1969) in the Um Bogma region, and the Amudei Shelomo Formation of Weissbrod and Perath (1990) in Israel. Said and El-Kelani (1989) introduced the name 'Taba Formation' to this unit, which is inconvenient because it represents the lower part of the Araba Formation in the type locality (Fig. 8).

The middle unit reflects intertidal to subtidal deposition and is associated with carbonate-dominated beds and trilobite tracks. The carbonate-dominated facies is not present in the Um Bogma region (Abdel-Motelib, 1996). This unit is equivalent to the Timna Formation of Weissbrod and Perath (1990) in Israel. The Timna Formation and the equivalent carbonate facies in Jordan are characterised by Cu, Mn and U mineralisation (Basta and Sunna, 1970; Khoury, 1986; Bar-Matthews, 1987). The middle unit is overlain by a shale-dominated unit deposited in an inner shelf environment. The middle and upper units are equivalent to the Abu Hamata Formation of Soliman and El-Fetouh (1969) in the Um Bogma area, and the Abu Hamata and Nasib Formations of Kora (1984) and El-Shahat and Kora (1986) in the same region (Fig. 8). The upper shale-dominated unit is equivalent to the Shehoret Formation of Weissbrod and Perath (1990) in Israel. This unit in the Um Bogma area, southwest of the study area, contains stratiform malachite deposits (El-Sharkawi *et al.*, 1990).

The stratiform malachite deposits are related to leaching products of Cu sulphides from Cu mineralised Precambrian rocks of the Arabo-Nubian Shield of the surrounded borders in Jordan (Burgath *et al.*, 1984) and Sinai (El-Shazly *et al.*, 1955). Kora (1991) subdivided the Palæozoic strata in the Taba region into the Sarabit El-Khadim, Abu Hamata and Adedia Formations (Fig. 8) of Cambro-Silurian age. Subsequently, Kora (*op. cit.*) subdivided the Abu Hamata Formation into the lower Ras El-Naqab Member and the upper Nasib Member.

DEPOSITIONAL HISTORY AND CONCLUSION

Vertical and lateral stacking of the depositional facies of the Araba Formation in the Taba region provide evidence of an overall retrogradational trend and a relative rise in sea level. The deposition of the Araba Formation records the transition from a fluvial regime at the basal part of the formation to intertidal-subtidal and shelf environments at the middle and upper parts, respectively. The recorded sea level changes during the Araba Formation sedimentation reflect a strong tectonic control and eustatic influence, which prevailed during the Early Palæozoic in northern Egypt and adjacent areas (Keeley, 1994).

Facies associations of unit I indicate deposition within low sinuosity braided channels associated with floodplain and alluvial fan deposits. They are chiefly composed of pebbly coarse-grained sandstones which are characterised by tabular cross-bedding and horizontal stratification. Channel deposits are believed to reflect the relative proximity to a source area. Floodplain fines consist of dark shales, mudstones and fine-grained sandstones with occasional bioturbations and organic matter. The aggradation and progradation of floodplain deposits are controlled by oscillations in river discharge.

The depositional facies of unit II point to a landward migration of the shoreline. The main components of this unit comprises fine- to coarse-grained sandstones, thin mudstone and shale intercalations. They reflect an upper to lower shoreface suite and tidal channel deposits. Despite the deepening-upward tendency of unit II, facies IIb marks a step forward in the progradation and an interruption of the relative sea level rise. Facies IIb is dominated by intercalations of dolostones, sandstones and shales. They indicate upper to middle intertidal flat. The relative sea level fall and subærial exposure of facies IIb are documented by the presence of karstification, brecciation, fresh water sparry calcite fillings, dedolomitisation, bioturbations and terra rossa development.

The shale-dominated succession of unit III points to a pronounced sea transgression and the creation of more space into which thick, fine-grained inner shelf deposits are introduced. Within this sequence, a progradational-upward trend is recognised in the transition from facies IIIa, of a deep inner shelf suite, to facies IIIb, of shallow inner shelf conditions. This is concomitant with an increase in the percentage of the interbedded fine-grained sandstones. They mostly reveal a wavy contact with associated shales. The overlying Naqus Formation displays an increase in the coarse-grained siliciclastic input and a contemporaneous eustatic sea level fall.

ACKNOWLEDGEMENTS

The authors are grateful to Prof. A.M. Abou Khadrah, Geology Department, Cairo University, Egypt, for his stimulating discussions.
Editorial handling - T. Weisbrod

REFERENCES

Abdallah, A.M., 1992. Palaeozoic rocks in Egypt. Technika Poszukiwan Geologicznych. Geosynoptyka Geotermina 3, 1–12.

Abdel-Khalek, M.L., Abdel-Wahed, M., Sehim, A.A., 1992. Gravitational tectonics in the northwestern part of the Gulf of Aqaba, Sinai, Egypt. In: Sadek, A. (Ed.), 1st International Conference of Geology of the Arab World, Cairo University, Egypt, pp. 395–415.

Abdel-Khalek, M.L., Abdel-Wahed, M., Sehim, A.A., 1993. Wrenching deformation and tectonic setting of northwestern part of the Gulf of Aqaba. Geological Society Egypt, Special Publication 1, 409–444.

Abdel-Motelib, A., 1996. Geological and mineralogical studies of some manganese occurrences of Egypt. Ph.D. dissertation, Cairo University, Egypt, 304p.

Abed, A.M., Makhlouf, I.M., Amireh, B.S., Khalil, B., 1993. Upper Ordovician glacial deposits in southern Jordan. Episodes 16, 316–328.

Ainsowrth, R.B., Crowley, S.F., 1994. Wave-dominated nearshore sedimentation and 'forced' regression: Post-abondonment facies, Great Limestone Cyclothem, Stainmore, UK. Journal Geological Society London 151, 681–696.

Allam, A., 1989. The Palaeozoic sandstones in Wadi Feiran - El-Tor area, Sinai, Egypt. Journal African Earth Sciences 9, 49–57.

Ball, J., 1916. The geography and geology of west central Sinai, Egypt. Survey Deptartment, Cairo, 219p.

Bar-Matthews, M., 1987. The genesis of uranium in manganese and phosphorite assemblages, Timna Basin, Israel. Geological Magazine 124, 211–229.

Barron, T., 1907. The topography and geology of the peninsula of Sinai (Western Portion), Egypt. Survey Deptartment, Cairo, 241p.

Basta, E.Z., Sunna, B.F., 1970. The Manganese mineralisation at Feinan District, Jordan. Faculty Science Bulletin, Cairo University 111–126.

Bauerman, H., 1869. Note on a geological reconnaissance made in Arabia Ptraea in the spring of 1869. Journal Geological Society London 25, 17–38.

Beleity, A., Ghoneim, M., Hinawi, M., Fathi, M., Gebali, H., Kamel, M., 1986. Palaeozoic stratigraphy, paleogeography and paleotectonics in the Gulf of Suez. E.G.P.C: 8th Exploration Conference, Cairo, 21p.

Bhattacharyya, D.P., Dunn, L.G., 1986. Sedimentologic evidence for repeated pre-Cenozoic vertical movements along the northeast margin of the Nubian Craton. Journal African Earth Sciences 5, 147–153.

Burgath, K.P., Hagen, D., Siewers, V., 1984. Geochemistry, geology and primary copper mineralization in Wadi Araba, Jordan. Geologische Jahrbuch (B) 53, 3–53.

Chun, S.S., Chough, S.K., 1995. The Cretaceous Uhangari Formation, SW Korea: Lacustrine margin facies. Sedimentology 42, 293–322.

Collinson, J.D., 1996. Alluvial sediments. In: Reading, H.G. (Ed.), Sedimentary Environments: Processes, Facies and Stratigraphy. Blackwell Scientific Publications, London, pp. 37–82.

Einsele, G., 1992. Sedimentary basins. Springer-Verlag, Berlin, 628p.

El-Barkooky, A.N., 1992. Stratigraphic framework of the Palaeozoic in the Gulf of Suez region, Egypt. In: Abstract, 1st International Conference of Geology of the Arab World, Cairo University, Egypt.

El-Barkooky, A.N., 1996. Palaeozoic-Mesozoic boundary: its stratigraphical, sedimentological and paleontological implications in Sinai and Gulf of Suez. Ph.D. Dessertation, Cairo University, Egypt, 189p.

El-Kelani, A., 1996. Facies changes within the Early Palaeozoic in Sinai. In: Abstract, Geological Survey Egypt Centennial, Cairo, pp. 57–58.

El-Shahat, A., Kora, M., 1986. Petrology of the Early Palaeozoic rocks of Um Bogma area, Sinai. Mansoura Science Bulletin 13, 151–184.

El-Sharkawi, M.A., El-Aref, M.M., Abdel-Motelib, A., 1990. Syngenetic and paleokarstic copper mineralization in the Palaeozoic platform sediments of west central Sinai, Egypt. Special Publications International Association Sedimentogists 11, 159–172.

El-Shazly, E.M., Abdel-Naser, S., Shukri, B., 1955. Contibutions to the mineralogy of copper deposits in Sinai. Geological Survey Egypt Bulletin 1, 13p.

Geological map of Sinai, 1994. Geological Survey, Egypt. Sheet No. 2, scale 1:250 000.

Hassan, A.A., 1967. A new Carboniferous occurrence in Abu Durba, Sinai, Egypt. 6th Arab Petroleum Congress, Baghdad, 2, 8p.

Horton, B.K., Schmitt, J.G., 1996. Sedimentology of a lacustrine fan-delta system, Miocene Horse Camp Formation, Nevada, USA. Sedimentology 43, 133–155.

Husseini, M., 1991. Tectonic and depositional model of the Arabian and adjoining plates during the Silurian-Devonian. Bulletin American Association Petroleum Geologists 75, 108–120.

Issawi, B., Jux, U., 1982. Contributions to the stratigraphy of the Palaeozoic rocks in Egypt. Geological Survey Paper 64, 1–28.

Johnson, H.D., Baldwin, C.T., 1996. Shallow clastic seas. In: Reading, H.G. (Ed.), Sedimentary Environments: Processes, Facies and Stratigraphy. Blackwell Scientific Publications, London, pp. 232–280.

Keeley, M.L., 1994. Phanerozoic evolution of the basins of Northern Egypt and adjacent areas. Geologische Rundschau 43, 728–742.

Kenny, R., 1992. Origin of disconformity dedolomite in the Martin Formation (Late Devonian, northern Arizona). Sedimentary Geology 78, 137–146.

Khoury, H.N., 1986. On the origin of stratabound copper-manganese deposits in Wadi Araba, Jordan. Dirasat 13, 227–247.

Klitzsch, E., 1990. Palaeozoic. In: Said, R. (Ed.), The Geology of Egypt. Balkama, Rotterdam, pp. 393–406.

Kora, M., 1984. The Palaeozoic outcrops of Um Bogma area, Sinai. Ph.D. dissertation, Mansoura University, Egypt, 280p.

Kora, M., 1991. Lithostratigraophy of the Early Palaeozoic succession in Ras El Naqab area, east-central Sinai, Egypt. Newsletters Stratigraphy 24, 45–57.

Kostandi, A.B., 1959. Facies maps for the study of the Palaeozoic and Mesozoic sedimentary basins of the Egyptian region. In: 1st Arab Petroleum Congress,Cairo, 2, pp. 54-62.

McBride, E.F., Abdel-Waheb, A., Salem, A.M.K., 1996. The influence of diagenesis on the reservoir quality of Cambrian and Carboniferous, southwest Sinai, Egypt. Journal African Earth Sciences 22 (3), 285–300.

Miall, A.D., 1977. A review of the braided river depositional environment. Earth Science Reviews. 13, 1–62.

Miall, A.D., 1985. Architectural-element analysis: a new method of facies analysis applied to fluvial deposits. Earth Science Reviews 22, 261–308.

Morgan, P., 1990. Egypt in the framework of global tectonics. In: Said, R. (Ed.), The Geology of Egypt. Balkama, Rotterdam, pp. 91–111.

Morrow, D.W., 1982. Dolomite -part 2. Dolomitization models and ancient dolostones. Geoscience Canada 9, 95–107.

Omara, S., 1972. An early Cambrian outcrop in south western Sinai, Egypt. Neus Jahrbuch Geologie Paläontologie 5, 306–314.

Pettijohn, E.J., Potter, P.E., Siever, R., 1973. Sand and Sandstones. Springer-Verlag, Berlin, 617p.

Prave A.R., Duke, W.L., Slattery, W., 1996. A depositional model for storm- and tide-influenced prograding siliciclastic shorelines from the Middle Devonian of the central Applachian foreland, basin, USA. Sedimentology 43, 611–629.

Reading, H.G., 1981. Sedimentary environments and facies. Elsevier, New York, 544p.

Reineck, H.E., Singh, I.B., 1972. Genesis of laminated sand and graded rhythmites in storm-sand layers of shelf mud. Sedimentology 18, 123–128.

Reineck, H.E., Singh, I.B., 1980. Depositional sedimentary environments. Springer-Verlag, Berlin, 551p.

Rupple, S.C., Cander, H.S., 1988. Dolomitization of Shallow-water platform carbonates by sea water and seawater-derived brines: San Andres Formation (Guadalupian), West Texas. Society Economic Palæontologists Mineralogists, Special Publication 43, 245–262.

Said, M., El-Kelani, A., 1988. Contribution to the geology of southeast Sinai. In: 26th annual meeting of the Geological Society of Egypt, Cairo, pp. 30–31.

Said, R., 1971. Explanatory note to accompany the Geologic Map of Egypt. Geological Survey Egypt Paper 56, 121p.

Seilacher, A., 1990. Palaeozoic trace fossils. In: Said, R. (Ed.), The Geology of Egypt. Balkama, Rotterdam, pp. 646–670.

Semtner, A.K., Klitzsch E., 1994: Early Palaeozoic paleogeography of the northern Gondwana margin: new evidence for Ordovician-Silurian glaciation. Geologische Rundschau 83, 743–751.

Soliman, M.S., El-Fetouh, M.A., 1969. Petrology of the Carboniferous Sandstones in West Central Sinai. Journal Geology United Arab Republic 13, 61–143.

Stern, R.J., Kroner, A., 1993. Late Precambrian crustal evolution in NE Sudan: isotopic and geochronologic constraints. Journal Geology 101, 555–574.

Theriault, F., Hutcheon, I., 1987. Dolomitization and calcitization of the Devonian Grosmont Formation, Northern Alberta. Journal Sedimentary Petrology 57, 955–966.

Topographic map of Sinai, 1952. Egyptian Survey Corporation. Wadi Watir sheet, Sinai, Egypt, scale 1:100 000.

Tucker, M.E., Wright, V.P., 1990. Carbonate sedimentology. Blackwell Scientific Publications, Oxford, 482p.

Weissbrod, T., 1969. The Palaeozoic of Israel and adjacent countries. Israel Geological Survey Bulletin 47, 34p.

Weissbrod, T., Perath, I., 1990. Criteria for the recognition and correlation of sandstone in Precambrian and Palaeozoic-Mesozoic clastic sequence in the Near East. Journal African Earth Sciences 10, 253–270.